



Use of activated silica sol as a coagulant aid to remove aluminium from water defluoridated by electrocoagulation

Richa Sinha, Sanjay Mathur*

Department of Civil Engineering, Malaviya National Institute of Technology, Jaipur 302017, India, Tel. +91 7877290494; email: richamnit10@gmail.com (R. Sinha), Tel. +91 9549654213; email: smathur.ce@mnit.ac.in (S. Mathur)

Received 4 June 2015; Accepted 7 August 2015

ABSTRACT

Presence of fluorides in drinking water has become a public health problem. Aluminium compounds are popular for defluoridation of water owing to high affinity of fluoride toward aluminium. Use of these compounds may lead to high aluminium concentrations in drinking water. Aluminium is found to be a potential neurotoxicant. Synergistic associations of both aluminium and fluorides in the drinking water supply have been expounded by researchers. Aluminium–fluoride complexes also increase the risk of developing Alzheimer’s disease. Therefore, it is imperative to control the residual aluminium in the water. In the present work, the electrocoagulation process with aluminium electrodes has been used for defluoridation of water. In subsequent steps, activated silica sol has been used as a coagulant aid to remove aluminium from defluoridated water. Taguchi design has been used to develop a statistical model for aluminium removal. The experimental investigations revealed that activated silica sol reduces residual aluminium to a range of 0.003–0.034 mg/L.

Keywords: Activated silica sol; Aluminium; Coagulant aid; Electrocoagulation; Fluoride

1. Introduction

Fluoride in drinking water is a matter of concern in present time. A study by UNICEF shows that fluorosis is widespread in at least 27 countries across the globe [1]. Problems associated with excessive or prolonged exposure to fluoride contaminated drinking water may cause dental or skeletal fluorosis. In dental fluorosis, excessive fluoride can cause yellowing of teeth, white spots, and pitting or mottling of enamel [2]. Common symptoms of chronic fluoride exposure are skeletal fluorosis, which can lead to permanent bone and joint deformation [3]. Therefore, fluoride removal has been an issue of concern for environmental engineers for the

past few decades [2]. Aluminium-based compounds are useful adsorbent/coagulant for fluoride removal, owing to high affinity of fluoride toward aluminium [4]. Various treatment technologies have been developed for fluoride removal from drinking water using aluminium-based compounds. However, generation of large volume of sludge, hazardous waste categorization of metal hydroxides and high costs associated with chemical treatments have made them less acceptable [5].

Electrocoagulation (EC) process using aluminium electrodes is one such process for fluoride removal. Researchers [2,6–8] have demonstrated the effectiveness of EC with aluminium electrodes for defluoridation. EC has been suggested as an alternative to conventional coagulation [9,10]. Reduced sludge production, no

*Corresponding author.

requirement for chemical handling and ease of operation are some of the advantages of this process [8] making it an exciting option for fluoride removal.

Aluminium is found to be a potential neurotoxicant, and medical research and epidemiological surveys suggest that dissolved aluminium entering the bloodstream may cause Alzheimer's disease, Lou Gehrig's disease and other forms of senile dementia, encephalopathy, bone mineralization disorders, etc. [11,12]. Researchers have reported that various bound forms of aluminium with fluoride and other inorganic/organic ions are toxic in nature. Synergistic effects of aluminium and fluorides and its role in Alzheimer's disease have also been expounded by Gauthier et al. [13] and Strunecka and Patocka [14]. Therefore, it is imperative to study the actual aluminium concentration in water which is treated with aluminium compounds for fluoride removal.

The present investigation relates to development of integral system for treating the fluoride-rich groundwater for human consumption, which aims to reduce fluoride concentration as well as controlling aluminium concentration in final water. This study is the extension of work done by Sinha et al. [15]. From the work of Sinha and co-workers [15], it is evident that with increase in energy input, aluminium content in water treated by EC also increases. This fact underlines the requirement to optimize the energy input. Further study reported that although flocculation and settling result in appreciable reduction of aluminium content in water, it is still more than permissible limit of aluminium in drinking water (0.2 mg/L) IS: 10500:2012 [16]. Use of coagulant aid for better settling and hence better removal of aluminium has been successfully attempted and reported by Sinha et al. [15]. Bentonite was used in the study by Sinha et al. [15] and reported an optimum dose of 2 g/L to bring down aluminium content below permissible level in final water. In this study, activated silica sol is used as coagulant aid which is found to be effective in controlling aluminium at a much lower dose than bentonite and also reduces the sludge volume. The fluorides have been effectively removed by the use of EC treatment, and in subsequent steps, aluminium was also controlled using activated silica sol as a coagulant aid.

2. Materials and methods

2.1. Fluoride removal

Batch EC reactor was used to remove fluoride from water prepared in the laboratory by mixing tap water with NaF and NaCl (2 mM). NaCl was added to

promote conductivity. The electrical conductivity of the prepared samples was measured and set in the range 0.99–1.01 mS/cm. Since aluminium hydroxide is an amphoteric hydroxide, pH is a sensitive factor for the formation of $\text{Al}(\text{OH})_3$ flocs. The solid $\text{Al}(\text{OH})_3$ is most prevalent between pH 6 and 8, and above pH 9, the soluble species are dominant [2]. Thus, the pH value of the sample was set to 6. A 2L batch reactor with aluminium electrodes (84 mm width, 71 mm height and 2.5 mm thickness) was used. Electrodes were connected to DC power supply in monopolar configuration. Fluoride was determined using ion selective method [17] with a fluoride selective electrode (Thermo Scientific Orion 5-Star meter, 9609BNWP fluoride electrode). Fig. 1 shows the experimental set-up for fluoride removal.

2.2. Aluminium removal

Aluminium was removed using two step strategy: Firstly, energy input was optimized for desired fluoride removal. Optimization of energy input allows only necessary amount of aluminium dissolution for desired fluoride removal and restricts unnecessary aluminium to get into the system. The aluminium in resultant water, even after energy optimization, was more than permissible limit for aluminium in drinking water (IS:10500:2012 [16]). Thus, in second step, activated silica sol was added as coagulant aid to promote coagulation for better settling.

Activated silica sol was added after EC process and mixed thoroughly for 1 min at 40 rpm. This was followed by 20 min flocculation at 10 rpm. Radial flow impeller of diameter 7.5 cm was used for stirring. The suspension was allowed to settle for 30 min. The supernatant was filtered (2.2 μm filter) and analysed for remaining aluminium. Aluminium concentration was measured using Thermo Scientific Atomic

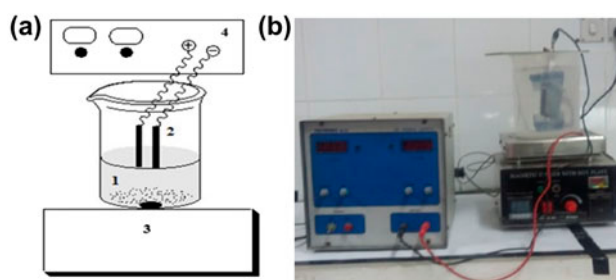


Fig. 1. Experimental set-up for fluoride removal. (a) Schematic diagram experimental setup 1: EC reactor, 2: Al electrodes, 3: magnetic stirrer and 4: DC power supply and (b) image of the experimental set-up of batch EC process.

Absorption Spectrophotometer (iCE 3000 series) with graphite furnace.

2.3. Particle size and turbidity measurement

Particle sizes in water sample after EC were measured to make a decision for further treatment. Turbidity of the samples after EC was also measured. Particle size was measured using Malvern Mastersizer-2000. Turbidity was measured using nephelometer of Electronics India.

2.4. Sludge characterization

The sludge was dried at 108–110°C for 12–18 h and then crushed to fine powder. The Fourier transform infrared spectroscopy (FTIR) measurements of activated silica sol and sludge were carried out using Perkin–Elmer Spectrum Two FTIR spectrometer. The X-ray diffraction (XRD) measurements of sludge were done using PANalytical X'Pert Powder.

3. Results and discussion

3.1. Implementation of Taguchi design

The study for fluoride removal was conducted using Taguchi method of design of experiments (MINITAB 14). The operating parameters studied were initial fluoride concentration (F) (2, 5 and 8 mg/L), applied current (i) (0.31, 0.53 and 0.75 A) and electrolysis time (t) (10, 30 and 50 min) for three responses: residual fluoride, residual aluminium and specific electrical energy consumption (SEEC). The data have been summarized in Table 1. The set of experiments suggested by Taguchi design was used to develop regression equations for mentioned responses. These equations were further used to optimize energy input for EC.

3.2. Optimization

The relationship between residual fluoride, residual aluminium and SEEC with combination of control factors is obtained using non-linear regression analysis with the help of SYSTAT 7.0 software as shown below in Eqs. (1)–(3). The data in Table 1 are normalized and used for developing the equations. The data are normalized by dividing each value with the maximum existing value in the column [18]. The equations obtained in the study for residual fluoride, residual aluminium and SEEC are presented in Eqs. (1–3), respectively.

$$\begin{aligned} \text{Residual fluoride} = & 0.608 + (0.741 \times F) - (0.557 \times i) \\ & - (1.3 \times t) - (0.559 \times F \times i) \\ & + (0.424 \times i \times t) - (0.622 \times F \times t) \\ & + (0.261 \times F^2) + (0.251 \times i^2) \\ & + (0.760 \times t^2) \end{aligned} \quad (1)$$

$$\begin{aligned} \text{Residual aluminium} = & 0.291 - (0.734 \times F) - (0.09 \times i) \\ & + (0.169 \times t) - (0.699 \times F \times i) \\ & + (0.709 \times i \times t) \\ & - (0.499 \times F \times t) + (0.765 \times F^2) \\ & + (0.315 \times i^2) + (0.094 \times t^2) \end{aligned} \quad (2)$$

$$\begin{aligned} \text{SEEC} = & 0.190 - (0.626 \times F) - (0.009 \times i) + (0.15 \times t) \\ & - (0.813 \times F \times i) + (0.628 \times i \times t) \\ & - (0.483 \times F \times t) + (0.608 \times F^2) + (0.4 \times i^2) \\ & + (0.024 \times t^2) \end{aligned} \quad (3)$$

In this study, Eq. (1) has been used to optimize the EC process for minimum energy input to achieve the target value of residual fluoride. The target value of residual fluoride was kept as 0.7 mg/L. IS:10500:2012 [16] recommends 1 mg/L as permissible limit of fluoride. In this study, target value of fluoride in treated water has been kept as 0.7 mg/L to take care of any possible error in prediction/measurement.

For optimization, a programme has been developed in FORTRAN using the technique of grid search method. The grid search method calculates the minimum point of a multivariable function using the grid search [18]. The multidimensional grid has a centroid which locates the optimum point. The search involves multiple passes. In each pass, the method locates a node (point of intersection) with the least function value. This node becomes the new centroid and builds a smaller grid around it. Successive passes end up shrinking the multidimensional grid around the optimum.

The objective of the programme was to obtain minimum applied current and electrolysis time for achieving target residual fluoride as 0.7 mg/L. Table 2 gives the details of sets optimized for energy input, which were determined with the help of FORTRAN programme. The value of minimum applied current and electrolysis time for each initial fluoride concentration was calculated by the programme and has been presented in Table 1 (Columns 3 and 4). The respective values for residual aluminium and SEEC were calculated by Eqs. (2) and (3) and have been presented in Table 1 (Columns 5 and 7, respectively).

Table 1
Orthogonal array for L27 (3^3) Taguchi design

S. no.	Operating parameters			Responses		
	Initial fluoride, F (mg/L)	Applied current, i (A)	Electrolysis time, t (min)	Residual fluoride (mg/L)	Residual Al (mg/L)	SEEC (J/mg)
1	2	0.31	10	1.12	9.4	454.43
2	2	0.31	30	0.31	19.48	709.88
3	2	0.31	50	0.23	28.12	1,129.66
4	2	0.53	10	0.71	10.6	776.51
5	2	0.53	30	0.36	26.12	1,832.37
6	2	0.53	50	0.09	47.04	2,622.25
7	2	0.75	10	0.61	14.9	1,392.08
8	2	0.75	30	0.18	33.48	3,182.56
9	2	0.75	50	0.01	48.5	4,861.81
10	5	0.31	10	1.56	6.2	116.25
11	5	0.31	30	0.71	12.1	279.39
12	5	0.31	50	0.29	18.05	424.52
13	5	0.53	10	1.42	7.81	279.8
14	5	0.53	30	0.25	17.5	632.65
15	5	0.53	50	0.19	27.6	1,041.27
16	5	0.75	10	1.27	9.25	518.76
17	5	0.75	30	0.14	25.8	1,194.44
18	5	0.75	50	0.11	39.45	1,978.52
19	8	0.31	10	3.40	6.07	86.93
20	8	0.31	30	1.35	10.53	180.41
21	8	0.31	50	0.60	17.5	270.2
22	8	0.53	10	2.30	6.53	175.74
23	8	0.53	30	0.56	15.79	403.91
24	8	0.53	50	0.30	25.75	650.45
25	8	0.75	10	1.37	10	291.85
26	8	0.75	30	0.38	23.68	762.21
27	8	0.75	50	0.23	40.42	1,245.65

Table 2
Details of optimized sets. (Minimum value of applied current and time for target value of residual fluoride as 0.7 mg/L)

Set no.	Operating parameters			Aluminium after EC (mg/L)		SEEC (J/mg)	
	Initial fluoride (mg/L)	Applied current (A)	Electrolysis time (min)	Predicted	Experimental	Predicted	Experimental
1	2	0.33	17.05	13.659	14.018	862.46	584.29
2	3	0.32	20.93	12.097	12.723	566.93	384.38
3	4	0.39	22.41	11.596	11.926	429.46	405.21
4	5	0.36	27.85	11.304	11.732	258.83	335.75
5	6	0.32	34.90	11.249	11.586	133.34	278.14
6	7	0.31	41.08	12.204	12.504	95.49	260.71
7	8	0.37	43.84	14.990	15.320	212.80	326.63

This optimization helps to restrict the unnecessary dissolution of aluminium and also offers better economics of the treatment.

3.3. Particle size and turbidity analysis

Particle size is an important parameter for flocculation studies [19]. Table 3 presents the results of particle size and turbidity, of the set no 1, 4 and 7 (Refer Table 1). $D(0.5)$, $D(0.1)$ and $D(0.9)$ are standard percentile readings from the analysis. $D(0.5)$ is the size in microns at which 50% of the sample is smaller and 50% is larger. $D(0.1)$ is the size of particle below which 10% of the sample lies. $D(0.9)$ is the size of particle below which 90% of the sample lies.

The high turbidity in the range of 21–54 NTU (Table 3) and high aluminium after EC with optimized energy input (Table 1) indicated requirement of further treatment. The turbidity is due to the aluminium complexes formed during the EC treatment for fluoride removal. The particle size of these flocs (Table 3) was less than 100 μm ; this indicates that flocculation and settling will be good choice to remove flocs [19]. It is known from the study of Sinha et al. [15] that these flocs contribute to the aluminium content in water and there is a requirement of coagulant aid to effectively settle them.

3.4. Coagulant aid

Activated silica sol was used as a coagulant aid in this study. Activated silica sol is a short chain polymer which is capable of binding aluminium hydrate particles used in coagulation processes. Activated silica sol is formed by polymerization of silicic acid which has no harmful effects on human health. Silicic acid has a strong and unique affinity for aluminium [20]. Evidence is accumulating, largely through the pioneering work of the late Birchall and co-workers [20–22], that silicic acid ($\text{Si}(\text{OH})_4(\text{aq})$) interacts with aqueous $\text{Al}(\text{III})$ so as to reduce the bioavailability (and hence the toxicity) of the latter. In humans, silicic acid seems to reduce gastrointestinal absorption of $\text{Al}(\text{III})$ and to

enhance its excretion through the kidneys [23,24]. Also few researches have reported that correlation of aluminium and Alzheimer's disease has led to the use of silicic acid in beverages [25], due to its abilities to both reduce aluminium uptake in the digestive system as well as cause renal excretion of aluminium.

3.5. Development of a statistical model

A statistical model was developed for the removal of aluminium from water using activated silica sol as a coagulant aid. The experimental study was designed using 4 level Taguchi design method ($L_{16} 2^4$). The operating parameters used were aluminium after EC (Al_{EC}) and activated silica sol dose (D_{as}) for the estimation of response (aluminium after activated silica sol dosing). Levels for the operating parameter " Al_{EC} " were selected from the results presented in Table 1 (Column 6). The minimum and maximum values of aluminium were used as Levels 1 and 4. The values of Levels 2 and 3 were chosen between these two extreme values. The levels of operating parameters have been presented in Table 4. MINITAB 14 software was used for the analysis of results. Sixteen experiments were performed in duplicate runs to determine residual aluminium (response parameter), and average readings have been presented in Table 5. The input settings for Taguchi design with respective response and signal-to-noise (S/N) ratio are presented in Table 5. The response values were transformed into S/N ratios. Various types of S/N ratios are used in the Taguchi method to measure variability around the target performance [26,27]. But the aim of the study was to reduce the aluminium content in the water, so the selected quality performance is "smaller the better" and its S/N is calculated as shown in Eq. (4).

$$S/N = -10 \log \frac{1}{n} \left(\sum_{i=1}^n y_i^2 \right) \quad (4)$$

where " n " is the number of tests and y_i is the value of experimental result, i.e. Al_{as} in the i th test. Higher values of the S/N ratio identify operating parameter settings that minimize the effects of the noise factors.

The results obtained in the Table 5 clearly indicate that activated silica sol effectively reduces the aluminium content below the permissible range of 0.2 mg/L (IS:10500:2012 [16]). To understand the mechanism of removal, it is necessary to study the surface groups present on the activated silica sol. Floc growth of activated silica sol with polymeric aluminium begins with the formation of negatively

Table 3
Particle size and turbidity for EC runs

Set no.	Particle size (μm)			Turbidity (NTU)
	$D(0.1)$	$D(0.5)$	$D(0.9)$	
1	4.282	13.306	24.488	21
4	4.244	14.386	45.721	32
7	6.186	21.496	62.410	54

Table 4
Levels used for operational parameters

Parameters	Notation	Units	Level 1	Level 2	Level 3	Level 4
Aluminium after EC	Al_{EC}	mg/L	11.586	12.723	14.018	15.320
Activated silica sol dose	D_{as}	mg/L	10	30	50	70

Table 5
Orthogonal array for L16 (2^4) Taguchi design

Set no.	Operating parameters			S/N ratio
	Aluminium after EC Al_{EC} (mg/L)	Activated silica sol dose	Aluminium after activated silica sol dosing Al_{as} (mg/L)	
1	11.586	10	0.056	25.036
2	11.586	30	0.003	50.457
3	11.586	50	0.015	36.478
4	11.586	70	0.062	24.152
5	12.723	10	0.077	22.270
6	12.723	30	0.018	34.894
7	12.723	50	0.03	30.457
8	12.723	70	0.08	21.938
9	14.018	10	0.089	21.012
10	14.018	30	0.029	30.752
11	14.018	50	0.037	28.635
12	14.018	70	0.085	21.411
13	15.320	10	0.095	20.445
14	15.320	30	0.034	29.370
15	15.320	50	0.045	26.935
16	15.320	70	0.093	20.630

Table 6
ANOVA table for residual aluminium after activated silica sol dosing

Source	DF	Seq SS	Adj SS	Adj MS	F	P
Aluminium after EC	3	219.63	219.63	73.21	11.38	0.002
Activated silica sol dose	3	853.47	853.47	284.49	44.24	0.000
Error	9	57.88	57.88	6.43		
Total	15	1,130.98				

$S = 2.53598$ $R^2 = 94.88\%$

charged aluminosilicate sites. When aluminium polycations approach silanol groups, aluminosilicate sites are formed which are negatively charged. This negative charge arises as aluminium changes its coordination from 6-fold to 4-fold upon contact with the silica tetrahedral structure [28]. These sites are similar to those found in clay minerals and zeolitic materials [29], which are supposed to be potential anchors to aluminium polycations. Newly created aluminosilicate

sites cause destabilization as a lot of negatively charged sites have been created. Charge compensation of these sights is done by the aluminium polycations. Aluminium polymers are expected to remain in the vicinity of the silica surface after reaction and represent the principal cations available for charge balance. Hence, aggregation of silica particles proceeds with either charge neutralization or bridging [30]. In the process of forming activated silica sol, silanol groups

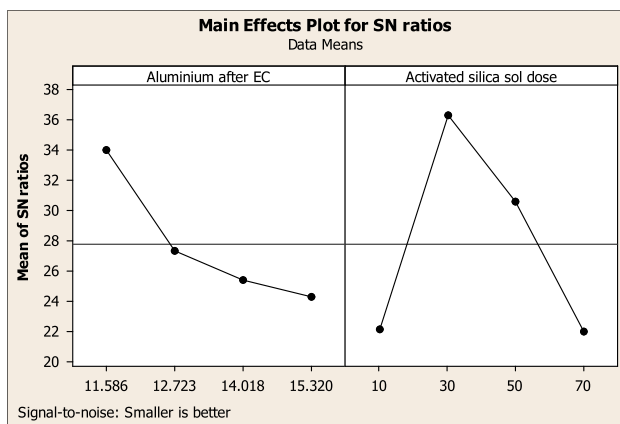


Fig. 2. Main effect plot for residual aluminium after activated silica dosing.

are formed on the silica surface in the course of its synthesis during the condensation-polymerization of $\text{Si}(\text{OH})_4$ [31]. It is generally agreed that the aluminosilicate sites are formed by condensation of the silanol groups present on the silica surface with the hydroxyl groups of the hydrolyzed aluminium ions [29,32]. Thus, efficient removal of aluminium takes place from the solution.

3.5.1. Validation of the model and main effect plots

The model is validated by ANOVA results. High R^2 value of 94.88% suggests toward the validity of the

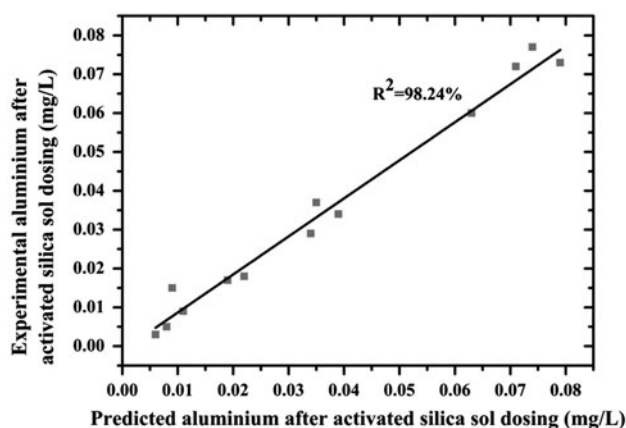


Fig. 3. Actual vs. predicted values for aluminium after activated silica dosing.

model as shown in Table 6. In ANOVA, "DF" is degree of freedom and implies to the number of values in final calculation of a statistic that are free to vary. "SS" is sum of squares which is an interim quantity used to study the population variance. "MS" is mean of a square which is obtained by dividing "SS" by DF. F -value is the ratio of mean squares calculated by dividing respective "MS" value with error. p -value determines the significance of the results. S is measured in the units of the response variable and represents the standard deviation of how far the data values fall from the fitted values. The lower the value of S , the better the model describes the response.

Table 7

Operational parameter settings and their respective actual and predicted responses selected for verification of regression equations

S. no.	Operational parameters		Aluminium after activated silica sol dosing (mg/L)	
	Aluminium after EC (mg/L)	Activated silica sol dose (g/L)	Predicted	Experimental
1	11.586	30	0.006	0.003
2	11.586	50	0.009	0.015
3	12.723	10	0.074	0.077
4	12.723	70	0.079	0.073
5	12.723	30	0.022	0.018
6	14.018	30	0.034	0.029
7	14.018	50	0.035	0.037
8	15.320	30	0.039	0.034
9	11.732	30	0.008	0.005
10	11.926	30	0.011	0.009
11	12.504	30	0.019	0.017
12	12.723	70	0.079	0.073
13	12.504	10	0.071	0.072
14	11.926	10	0.063	0.060

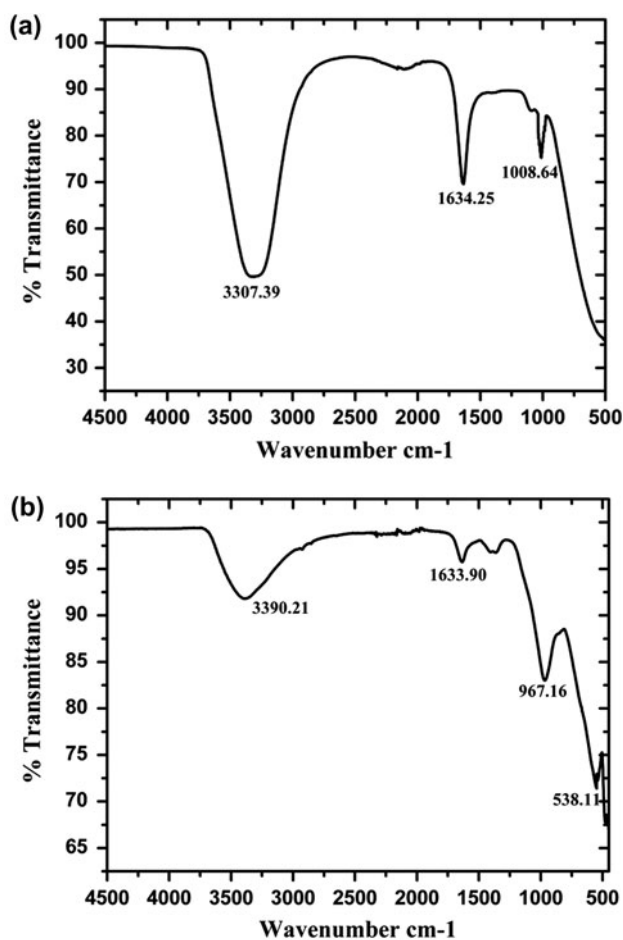


Fig. 4. FTIR scans for (a) activated silica sol (b) sludge after activated silica sol dosing.

The main effect plot is presented in Fig. 2. Fig. 2 explains that as the activated silica sol dose increases from 10 to 30 mg/L, the residual aluminium decreases, but further increase in activated silica sol dose from 30 to 50 mg/L results in the increase in the residual aluminium. So it can be clearly observed that 30 mg/L is the optimum dose for the performed experiments.

3.6. Development of regression equation and its verification

Sixteen experiments, presented in Table 5, were used to develop regression equation using SYSTAT 7.0 software. The regression equation to determine residual aluminium after activated silica sol dosing is shown in Eq. (5).

$$\begin{aligned} Al_{as} = & -3.815 + (10.153 \times Al_{EC}) - (3.588 \times D_{as}) \\ & - (0.458 \times Al_{EC} \times D_{as}) - (4.833 \times Al_{EC}^2) \\ & + (3.507 \times D_{as}^2) \end{aligned} \quad (5)$$

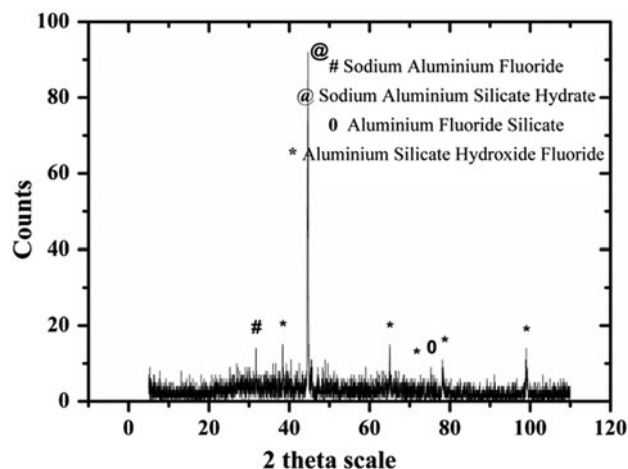


Fig. 5. XRD analysis of sludge produced in the treatment process after activated silica sol dosing.

Fourteen set of experiments were performed to verify correctness of Eq. (5). The results have been presented in Table 7. High R^2 value of 98.24%, as shown in Fig. 3, suggests the fitness of equation.

4. Sludge characterization

FTIR scans were conducted for activated silica sol and the sludge formed after treatment to understand the aluminium removal mechanisms. FTIR scans of activated silica sol (Fig. 4(a)) peaks at 3307.39 and 1634.25 cm^{-1} correspond to H–O–H bond stretching and H–O–H bending, respectively. FTIR scans of sludge (Fig. 4(b)) peaks at 3390.21 and 1633.90 cm^{-1} correspond to H–O–H bond stretching and H–O–H bending, respectively. The results corroborate the findings of Hayati-Ashtiani [33]. Si–O stretching bond peak was found at 1008.64 cm^{-1} for activated silica sol and at 967.16 cm^{-1} for sludge. These findings are in line with Stubican and Roy [34]. The presence of Si–O–Al peak at 538.11 cm^{-1} [34] is found in the scans of sludge. The formation of aluminosilicates indicates the role of activated silica sol in the removal of aluminium from the solution.

4.1. X-ray diffraction

The sludge remaining after the treatment was characterized by XRD (Fig. 5). Sodium aluminium silicate hydrate ($\text{NaAlSi}_2\text{O}_6 \cdot 3\text{H}_2\text{O}$), aluminium fluoride silicate ($\text{Al}_2(\text{SiO}_4)\text{F}_2$) and aluminium silicate hydroxide fluoride ($\text{Al}_2\text{SiO}_4((\text{OH})_{0.43}\text{F}_{1.57})$) were formed during Al(III) removal by the activated silica sol. Sodium aluminium fluoride ($\text{Na}_3(\text{AlF}_6)$) was formed during the

fluoride removal by EC process. The presence of these compounds indicates toward the chemisorption of aluminosilicate complexes to activated silica sol and verifies the role of activated silica sol as coagulant aid for the removal of aluminium from water treated by EC.

5. Conclusion

This study is focussed on aluminium removal from water defluoridated by the EC process. After EC treatment, aluminosilicate complexes are present in water. These flocs contribute to the aluminium content in water. Coagulation and settling could not settle these flocs efficiently, which leads to high aluminium content in water. It was found from this study that addition of coagulant aid assists in effective settling of flocs. In this study, activated silica sol has been successfully used as a coagulant aid to improve settling of flocs. Activated silica sol dose of 30 mg/L brings down residual aluminium to a much lower range of 0.003–0.034 mg/L.

References

- [1] N. Drouiche, S. Aoudj, H. Lounici, H. Mahmoudi, N. Ghaffour, M.F.A. Goosen, Development of an empirical model for fluoride removal from photovoltaic wastewater by electrocoagulation process, *Desalin. Water Treat.* 29 (2011) 96–102.
- [2] R. Sinha, A. Singh, S. Mathur, Multiobjective optimization for minimum residual fluoride and specific energy in electrocoagulation process, *Desalin. Water Treat.* (2014) 1–11. doi:10.1080/19443994.2014.990929.
- [3] K. Singh, D.H. Lataye, K.L. Wasewar, C.K. Yoo, Removal of fluoride from aqueous solution: Status and techniques, *Desalin. Water Treat.* 51 (2013) 3233–3247.
- [4] C.J. Huang, J.C. Liu, Precipitate flotation of fluoride-containing wastewater from a semiconductor manufacturer, *Water Res.* 33 (1999) 3403–3412.
- [5] A. Mazighi, H. Lounici, N. Drouiche, R. Leenaerts, N. Abdi, H. Grib, N. Mameri, Economic study of groundwater defluoridation of the North African Sahara, *Desalin. Water Treat.* 54 (2015) 2681–2691.
- [6] N. Drouiche, H. Lounici, M. Drouiche, N. Mameri, N. Ghaffour, Removal of fluoride from photovoltaic wastewater by electrocoagulation and products characteristics, *Desalin. Water Treat.* 7 (2009) 236–241.
- [7] S. Aoudj, A. Khelifa, N. Drouiche, M. Hecini, HF wastewater remediation by electrocoagulation process, *Desalin. Water Treat.* 51 (2013) 1596–1602.
- [8] M.M. Emamjomeh, M. Sivakumar, Fluoride removal by a continuous flow electrocoagulation reactor, *J. Environ. Manage.* 90 (2009) 1204–1212.
- [9] C.-Y. Hu, S.-L. Lo, W.-H. Kuan, Simulation the kinetics of fluoride removal by electrocoagulation (EC) process using aluminum electrodes, *J. Hazard. Mater.* 145 (2007) 180–185.
- [10] J. Zhu, H. Zhao, J. Ni, Fluoride distribution in electrocoagulation defluoridation process, *Sep. Purif. Technol.* 56 (2007) 184–191.
- [11] C.N. Martyn, D.J.P. Barker, C. Osmond, E.C. Harris, J.A. Edwardson, R.F. Lacey, Geological relation between Alzheimer's disease and aluminium in drinking water, *The Lancet* 1 (1989) 59–62.
- [12] D.R. Mc Lachlan, T.P. Kruck, W.J. Lukiw, S.S. Krishnan, Would decreased aluminum ingestion reduce the incidence of Alzheimer's disease? *Can. Med. Assoc. J.* 145 (1991) 793–804.
- [13] E. Gauthier, I. Fortier, F. Courchesne, P. Pepin, J. Mortimer, D. Gauvreau, Aluminum forms in drinking water and risk of Alzheimer's disease, *Environ. Res.* 84 (2000) 234–246.
- [14] A. Strunecka, J. Patocka, Pharmacological and toxicological effects of aluminofluoride complexes, *Fluoride* 32 (1999) 230–242.
- [15] R. Sinha, S. Mathur, U. Brighu, Aluminium removal from water after defluoridation with electrocoagulation process, *Environ. Technol.* (2015). doi:10.1080/09593330.2015.1043958.
- [16] Bureau of Indian standards, Indian Standard—Drinking Water Specification, second revision, 2012.
- [17] L.S. Clesceri, A.E. Greenberg, A.D. Eaton (Eds.), *Standard Methods for the Examination of Water and Wastewater*, twentieth ed., APHA-AWWA-WEF, Washington, DC, 1998.
- [18] R. Sinha, S. Mathur, Control of aluminium in treated water after defluoridation by electrocoagulation and modelling of adsorption isotherms, *Desalin. Water Treat.* (2015). doi:10.1080/19443994.2015.1060538.
- [19] B.M. Moudgil, S. Behl, T.S. Prakash, Effect of particle size in flocculation, *J. Colloid Interface Sci.* 158 (1993) 511–512.
- [20] J.D. Birchall, C. Exley, J.S. Chappell, M.J. Phillips, Acute toxicity of aluminium to fish eliminated in silicon-rich acid waters, *Nature* 338 (1989) 146–148.
- [21] J.D. Birchall, J.S. Chappell, Aluminium, water chemistry, and Alzheimer's disease, *The Lancet* 333 (1989) 953.
- [22] J.D. Birchall, D. Chadwick, J. Whelan (Eds.), *Aluminum in Biology and Medicine*, vol. 169, John Wiley and Sons, New York, NY, 1992.
- [23] J.D. Birchall, J.P. Bellia, N.B. Roberts, On the mechanisms underlying the essentiality of silicon—Interactions with aluminium and copper, *Coord. Chem. Rev.* 149 (1996) 231–240.
- [24] D.M. Reffitt, R. Jugdaohsingh, R.P.H. Thompson, J.J. Powell, Silicic acid: Its gastrointestinal uptake and urinary excretion in man and effects on aluminium excretion, *J. Inorg. Biochem.* 76 (1999) 141–147.
- [25] C. Exley, C. Schneider, F.J. Doucet, The reaction of aluminium with silicic acid in acidic solution: An important mechanism in controlling the biological availability of aluminium? *Coord. Chem. Rev.* 228 (2002) 127–135.
- [26] M.S. Phadke, *Quality Engineering Using Robust Design*, PTR Prentice Hall, Englewood Cliffs, NJ, 1989, pp. 100–120.
- [27] R.K. Roy, *A Primer on the Taguchi Method*, Society of Manufacturing Engineers, Ann Arbor, MI, 1990, pp. 145–154.
- [28] L. Pauling, *The Nature of the Chemical Bond*, third ed., Cornell University Press, Ithaca, NY, 1980, pp. 153–164.

- [29] P. Cloos, A.J. Leonard, J.P. Moresu, A. Herbillon, J.J. Fripiat, Structural organization in amorphous silico-aluminas, *Clays Clay Miner* 17 (1969) 279–287.
- [30] B.S. Lartiges, J.Y. Bottero, L.S. Derrendinger, B. Humbert, P. Tekely, H. Suty, Flocculation of colloidal silica with hydrolyzed aluminum: An ^{27}Al solid state NMR investigation, *Langmuir* 13 (1997) 147–152.
- [31] L.T. Zhuravlev, The surface chemistry of amorphous silica. Zhuravlev model, *Colloids Surf., A* 173 (2000) 1–38.
- [32] M.W. Tamele, Chemistry of the surface and the activity of alumina-silica cracking catalyst, *Discuss. Faraday Soc.* 8 (1950) 270–279.
- [33] M. Hayati-Ashtiani, Use of FTIR spectroscopy in the characterization of natural and treated nanostructured bentonites (montmorillonites), *Part. Sci. Technol.* 30 (2012) 553–564.
- [34] V. Stubican, R. Roy, Infrared spectra of layer-structure silicates, *J. Am. Ceram. Soc.* 44 (1961) 625–627.